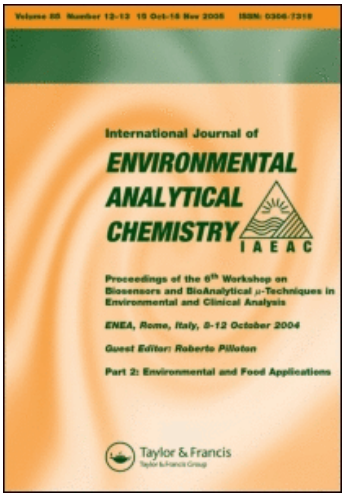

International Journal of Environmental Analytical Chemistry
Publication details, including instructions for authors and subscription information:
http://www.informaworld.com/smpp/title~content=t713640455

Evolution of anthropogenic aerosols in the coastal town of Salina Cruz, Mexico: part III size-segregated elemental composition analysed by total-reflection X-ray fluorescence spectrometry

Gerhard Lammel[a]; Darrel G. Baumgardner[b]; Ursula E. A. Fittschen[c]; Birgit Peschel[c]
[a] Max Planck Institute for Meteorology, 20146 Hamburg, Germany [b] Center for Atmospheric Sciences, Universidad Nacional Autónoma de México, Ciudad Universitaria, Mexico [c] University of Hamburg, Institute for Inorganic and Applied Chemistry, 20146 Hamburg, Germany

To cite this Article Lammel, Gerhard , Baumgardner, Darrel G. , Fittschen, Ursula E. A. and Peschel, Birgit(2007) 'Evolution of anthropogenic aerosols in the coastal town of Salina Cruz, Mexico: part III size-segregated elemental composition analysed by total-reflection X-ray fluorescence spectrometry', International Journal of Environmental Analytical Chemistry, 87: 9, 659 — 672
To link to this Article: DOI: 10.1080/03067310701321967
URL: http://dx.doi.org/10.1080/03067310701321967

Intern. J. Environ. Anal. Chem.
Vol. 87, No. 9, 10 August 2007, 659–672

Taylor & Francis
Taylor & Francis Group

Evolution of anthropogenic aerosols in the coastal town of Salina Cruz, Mexico: part III size-segregated elemental composition analysed by total-reflection X-ray fluorescence spectrometry

GERHARD LAMMEL*†, DARREL G. BAUMGARDNER‡, URSULA E. A. FITTSCHEN§ and BIRGIT PESCHEL§

†Max Planck Institute for Meteorology, Bundesstr. 53, 20146 Hamburg, Germany
‡Center for Atmospheric Sciences, Universidad Nacional Autónoma de México, Ciudad Universitaria, 04510 Mexico D.F., Mexico
§University of Hamburg, Institute for Inorganic and Applied Chemistry, 20146 Hamburg, Germany

(*Received 20 October 2006; in final form 6 March 2007*)

Heavy metals in various size modes of the atmospheric aerosol are a concern for human health. Their and other elements' concentrations are indicative for anthropogenic and natural aerosol sources. Si, Cl, K, Ca, Ti, V, Cr, Mn, Fe, Co, Ni, Cu, Zn, As, Se, Br, Rb, Sr, Hg, and Pb were determined as a complementary contribution to a study on aerosol cycling during the wet season, June 2004, in a humid, subtropical climate, i.e. in the city of Salina Cruz, situated on the Pacific coast of the Isthmus of Tehuantepec (16.2°N, 95.2°W), Mexico. For mass (gravimetry) and elemental analyses, particles were collected by a Berner low-pressure round nozzle cascade impactor using four stages corresponding to 0.1–0.25, 0.25–1.0, 1.0–4.0, and 4–16 μm of aerodynamic particle size. The impaction plates were modified such that approx. 1/6 consisted of a plastic support (Persplex®) for total reflection X-ray fluorescence spectrometry (TXRF). The elements' total content was determined by TXRF without any further sample pretreatment. Limits of quantification (LOQ) for elemental content in individual impactor stages corresponded to 25–60 ng m^{-3} for Si; 0.8–4 ng m^{-3} for Cl, K, Ca, Ti, and V; 3–20 pg m^{-3} for Cr, Mn, Fe, Cu, Ni, and Zn; and 7–50 pg m^{-3} for As, Se, Br, Rb, Sr, Hg, and Pb. In some samples, however, high blank values for the supports gave an LOQ = 6–19 ng m^{-3} for Cl; 3–7 ng m^{-3} for Ca; 3–7 ng m^{-3} for Fe, Ni, Cu, and Zn; and 60–70 ng m^{-3} for Pb. The influence of local natural, industrial, and vehicle traffic sources for heavy-metal mobilization was obvious. Heavy-metal abundances did not coincide with regionally distributed pollutants. V and Ni were found at particularly elevated levels advected with the sea breeze, which points to ships as sources. Br and Pb were found at particularly low levels. The concentrations of Br, Rb, Sr, and Pb were found below LOQ at least in some, As, Co, Se, and Hg in all of the samples. The elements' characteristic differences in mass size distributions were obvious despite the coarse size resolution. During the cycling of air masses from land to sea and back again, enrichment of super-micrometre particles in the near ground aerosol was observed under dry weather conditions. Rain preferentially removed the large particles with which heavy metals have been associated.

*Corresponding author. Fax: +49-40-41173-390. Email: gerhard.lammel@zmaw.de

International Journal of Environmental and Analytical Chemistry
ISSN 0306-7319 print/ISSN 1029-0397 online © 2007 Taylor & Francis
DOI: 10.1080/03067310701321967

Keywords: Total-reflection X-ray fluorescence spectrometry; Atmospheric aerosols; Heavy metals; Air pollution; Particle-size distribution; Subtropics

1. Introduction

Fine particulate matter influences cloud droplet formation, radiation (and, hence, climate), provides a medium for chemical transformations, and is hazardous to human health. Key parameters for all these implications are particle size and chemical composition. Although airborne concentrations are generally well below levels known to cause adverse health effects from inhalation exposure, the health impact from long-term exposure to elevated levels of fine particles seems to be severe (e.g. [1, 2]). The exact damaging agents of particles have not been identified, nor their pathophysiological mechanisms leading to disease are fully understood, but some heavy metals are a concern for human health in urban areas of Mexico and elsewhere (e.g. [3, 4]). Furthermore, the elemental content of the various modes of the aerosol size distribution is of interest, because it is indicative for aerosol sources and provides unique complementary information for source attribution (e.g. [5, 6]).

The mass mixing ratios of elements in atmospheric particulate matter (typically 10^{-6} to 10^{-3}), aerosol abundances (typically less than $0.1\,\mathrm{mg\,m^{-3}}$) together with the characteristics of sampling techniques and requirements with regard to time resolution (12 h and less) and particle-size resolution translate into a high demand for sensitivity of the analysis method. Total reflection X-ray fluorescence analysis (TXRF; e.g. [7, 8]) has been successfully applied for the analysis of total element contents of atmospheric particulate matter. Other multielemental methods require large (mg) amounts of particulate matter for analysis, and a separation step of the sample from the collection substrate, which is time-consuming and subject to risks of contamination and loss of analyte [9]. This applies to ICP-OES, ICP-MS, and AAS. Or, like photon-induced X-ray emission (PIXE), offer microanalysis (requiring less than a few micrograms) and analysis of the particles directly on the collection substrate, but require an accelerator facility for sample excitation. Due to its high sensitivity, TXRF is suitable for size-segregated aerosol analysis when spatially focused and homogeneous samples are collected [10, 11].

The aim of the measurements reported here was to test a sampling method for TXRF analysis and determine elements which are indicative for natural and anthropogenic sources and their major size modes of atmospheric particulate matter in an urban area in Mexico. To our knowledge, very few or no measurements of heavy metals in urban air in Mexico exist outside the capital metropolitan area. The measurements were part of a field study with the goal to study processes of aerosol dynamics and chemical composition in a polluted coastal environment of the subtropics in the wet season. Many coastal areas are densely populated and often heavily polluted. In tropical and sub-tropical climates, air pollutant removal mechanisms differ considerably from temperate climates. The other aspects of this study, not directly related to elemental composition, are published elsewhere [12, 13].

2. Experimental

2.1 *Sampling site*

The study was performed on 5–18 June 2004 in the city of Salina Cruz, situated on the Pacific coast of the Isthmus of Tehuantepec. The city, with approx. 200,000 inhabitants, has one of the country's largest oil refineries. The measurements took place close to the city centre on the premises of the Oceanographic Station of the Secretaria de Marina (16° 10′ 40″ N, 95° 11′ 44″ W) in a backyard, 15 m a.s.l., close to road traffic sources, south of the majority of vehicular traffic in the heavily populated areas, 1.5 km north of the coast (harbour) and 3 km south to south-west of a refinery, one of the largest facilities of its type in Mexico. Seen from the sampling site, the extension of the refinery covers the wind sector from 10° to 45°. No other significant industrial emission sources exist in the town or in its surroundings. A chain of small hills, with summits less than 100 m above surrounding terrain separate the city from the refinery [12].

2.2 *Sampling and analytical methods*

A coarse size resolution, with four size ranges, was chosen as it is sufficient to determine the distribution of elements over the major size modes, sub-micrometre (so-called accumulation mode) and super-micrometre (dominated by the coarse mode in the range 2.5–10 μm). We used a modified round-nozzle Berner low-pressure cascade impactor. This was used to sample $24 \pm 2\,\mathrm{L\,min^{-1}}$ from a flow conveyed by a 3-m-high chimney ventilated at a rate of $90\,\mathrm{L\,min^{-1}}$. The impactor flow was controlled several times per sampling interval, at least when sampling was started and stopped, using a calibrated flowmeter (Gilibrator, Gilian). The impactor was equipped with five stages corresponding to lower cutoffs of 16, 4.0, 1.0, 0.25, and 0.13 μm. Pump failure caused flow reduction and, correspondingly, a change in effective cutoffs during the periods 9.6, 10–18 h, and from 10.6. 10 h until 11.6. 18 h. These data are neglected in the following.

The lower four stages (1–4, 1 corresponding to smaller particle sizes) were analysed. The ring-formed steel impaction plates (with outer and inner diameters of 70 and 30 mm, respectively) were modified such that a small part, corresponding to a 70° sector of the ring, consisted of a plastic support (Persplex®) for total-reflection X-ray fluorescence analysis (TXRF). These are as thick as the rest of the ring, 3 mm, or thinner, 2 mm, but anyway placed in such a way that the level of the impaction side of the plate remained unchanged. Thus, 80% of the particulate matter samples were available for other analyses. The supports are removable. All plastic supports had been analysed prior to exposure by TXRF in their central area, i.e. the area accessible for the detector, approx. $3 \times 5\,\mathrm{mm^2}$. By covering the plastic supports with a tape (of which a central area of 8 mm by diameter had been punched out), only a small fraction of the area was exposed. The number of impaction spots in the exposed area varied with the number and density of nozzles across stages and was 1, 2, 1, and 5 for stages 4–1 (decreasing cutoffs), respectively. The total content of the elements Si, Cl, K, Ca, Ti, V, Cr, Mn, Fe, Co, Ni, Cu, Zn, As, Se, Br, Rb, Sr, Hg, and Pb was determined by TXRF using the K lines for all elements except Pb and Hg where the L lines were used, without any further sample pretreatment. Sc was added as an internal standard. Some light elements, Na, Mg, Al, P, and S, were detected but not quantified.

The limits of detection (LOD) of the element content in individual impactor stages were 15–40 pg (corresponding to $3–20\,\mathrm{pg\,m^{-3}}$) for Cr, Mn, Fe, Cu, Ni, and Zn;

0.1–10 ng (0.02–5 ng m^{-3}) for Si, Cl, K, Ca, Ti, and V; and 40–100 pg (7–50 pg m^{-3}) for As, Se, Br, Rb, Sr, Hg, and Pb. These were determined, considering the background generated count rate [14]. Based on the instrument's error analysis and replicate spectra, a precision of >75% is estimated for Ti, As, Se, Br, Sr, Hg, and Pb; >90% for Si, Cl, V, Cr, Mn, Fe, Co, and Rb; and >95% for K, Ca, Ni, Cu, and Zn.

Blank values based on analyses prior to exposure revealed a large variation. The reason for this remained unclear. According to purity, the plastic supports had been grouped into three classes, and the cleanest supports (class 1) had been preferentially used for impactor stages 2 and 3 (corresponding to the 0.25–4.0 μm size range). Class 3 was rejected and discarded. The atmospheric concentrations of the elements were determined whenever the blank signal read zero or if the TXRF signal of the element in the sample exceeded double the blank signal (determined prior to exposure) by more than 2 standard deviations of the sample signal. Otherwise, the sample was discarded as undetermined. In this case, no upper limit for element mass was derived. Many class 2 samples ended up 'undetermined'. Sample contamination by the impactor material did not occur to any measurable extent. It had been observed when sampling with a similar impactor [11]. We suspect that abrasion from the impactor walls declines considerably during impactor lifetime.

The limits of quantification, LOQ, were defined as:

$$\mathrm{LOQ} = 3 \times \mathrm{LOD} \quad \text{for } \mu + 3\sigma \leq 3 \times \mathrm{LOD}$$

$$\mathrm{LOQ} = \mu \quad \text{for } \mu + 3\sigma > 3 \times \mathrm{LOD},$$

with μ and σ being the mean and standard deviation of six field blanks that each of class 1 and class 2 supports. $\mu + 3\sigma$ of the field blanks corresponded to 0.01–0.03 ng for Fe and Cu and <0.01 ng for the heavier elements when class 1 supports were used (per individual impactor stage). These values are not far from $1 \times \mathrm{LOD}$. Contamination was significantly higher, however, for class 2 supports for some elements, namely 0.07 ng (corresponding to 0.01–0.03 ng m^{-3}) for Pb; 3–7 ng (0.6–3.4 ng m^{-3}) for Ca, Fe, Ni, Cu, and Zn; and 30 ng (6–14 ng m^{-3}) for Cl (per individual impactor stage). Large ranges for the LOQ, partly more than one order of magnitude, result for these elements. The ranges for LOQ values determined for complete samples (i.e. all four impactor stages, both classes of supports included) are listed in table 1.

The remaining part of the impaction plates, containing 80% of the sample, was covered by pre-weighed Al foils and used for gravimetry (microbalance): particulate mass concentrations were determined by pre- and post-weighing of Al foils (0.15 mm) equilibrated to a constant humidity (3 days, 54 ± 2%) with a microbalance. Field blank values did not deviate from 0. Values below the LOQ (32 ng = 2 standard deviations of the blank values, corresponding to 2–8 μg m^{-3}) were substituted by 0 for derivation of mean values.

Sampling losses due to bounce-off had been observed with this type of impactor. These are, however, determined by sampling substrate (i.e. material of the foil) and air humidity, and can be neglected under humid conditions (e.g. [15]; relative humidity 76 ± 10% and never <52% during this study).

Table 1. Summary of the particulate matter mass (PM_{16}), m, and elemental concentrations during the entire project ($n = 18$), day/night ratio ($n = 8$ and 10, respectively) and north to north-east/east to north-west wind sector ratio ($n = 4$ and 9, respectively).[a]

	n	LOQ	$\mu \pm \sigma$	Min–Max	μ_{day}/μ_{night}	$\mu_{rain}/\mu_{no\ rain}$[b]	$\mu_{northerly}/\mu_{southerly}$[c]
m	18	2.0–8.0	16.0 ± 14.2	7.1–53.3	1.7	0.6	1.3
Si	15	25–60	835 ± 591	78–2104	1.4	0.2	1.1
Cl	11	17–56	110 ± 64	25–210	1.1	1.0	0.5
K	17	3.7–8.8	131 ± 72	44–293	1.5	0.4	0.9
Ca	16	2.5–6.9	194 ± 114	64–440	1.5	0.4	0.6
Ti	15	1.9–4.8	21 ± 13	5.1–46	2.0	0.3	0.9
V	13	0.8–2.0	26 ± 42	1.4–152	8.6	0.2	0.2
Cr	3	0.05–0.12	0.9 ± 1.1	0.2–2.1	nd	nd	nd
Mn	16	0.10–0.23	4.9 ± 3.4	1.4–10.5	4.7	0.3	0.7
Fe	18	0.07–14	231 ± 132	69–511	1.5	0.5	0.9
Co	6	0.07–0.2	< 0.2				
Ni	7	0.10–8.1	9.8 ± 15.3	1.4–44	11	0.1	nd
Cu	7	0.05–13	14.2 ± 14.3	1.1–39	1.9	3.7	0.9
Zn	13	0.05–6.5	24 ± 22	3.3–85	1.8	0.8	nd
As	3	0.15–0.35	< 0.35				
Se	4	0.2–0.4	< 0.4				
Br	4	0.25–0.6	1.25 ± 0.57	<0.6–1.2	nd	1.2	nd
Rb	9	0.25–0.6	1.10 ± 0.92	<0.6–1.7	35	0.4	1.0
Sr	6	0.25–0.6	1.51 ± 0.57	<0.6–2.2	17	0.8	2.1
Hg	8	0.25–0.6	<0.6				
Pb	5	0.10–0.13	0.77 ± 0.34	<0.13–1.03	nd	2.0	nd

[a]LOQ = limit of quantification for four impactor stages (ng m^{-3} except m: μg m^{-3}). Data are given in the form arithmetic mean ± standard deviation ($\mu \pm \sigma$), minimum and maximum (min–max) in ng m^{-3} (except m: μg m^{-3}).
[b]Ratio of means of samples from periods with rain and without rain. $n \geq 2$ for each data subset.
[c]Ratio of means of samples from periods with advection dominated by the north to north-east wind sector (>60% of the time, $n = 9$) and dominated by southerly directions (i.e. >80%). $n \geq 2$ for each data subset.
nd: not determined.

3. Results and discussion

3.1 *Meteorological conditions*

During the measurement campaign, the region was continuously under the easterly flow characteristic for these latitudes. As a consequence, at the site, winds from the north-east across the Isthmus of Tehuantepec prevailed from around sunset to the morning hours (between 9:00 and 12:00), while the sea breeze from the south to south-east prevailed the rest of the day. In agreement with the seasonality of the winds in the region [16], northerly and southerly winds were almost similarly frequent (46 and 54% of the time, respectively) during the measurement period and the wind velocity at an annual low, 1.5 m s^{-1} on average. Day-time (10–18 h) and night-time (18–10 h) samples are collected separately. Heavy rain occurred on 4–5, 8–9, and 12 June. This was caused by easterly waves which reached Salina Cruz and stopped the sea breeze rhythm.

Additional information on meteorological parameters and advection to the site is given in the companion articles [12, 13].

3.2 *Mass concentrations and influences of possible sources*

The mean concentration values of the particulate phase elemental concentrations, i.e. the sum of the four stages for the entire project, 5–18 June, and of data subsets

stratifying according to day *versus* night, no rain *versus* rain, and northerly *versus* southerly advection, are listed in table 1. For many elements, the number of samples determined is much smaller than the total number of samples (18), because the concentration could not be determined in one or more of the impactor stages. Listed are the results from complete sets of determinations across the four impactor stages as well as sets consisting of determinations from three stages, when either impactor stage 1 or 4 (those with the lowest concentrations), but not both, could not be determined. The concentrations of Br, Rb, Sr, and Pb were found below LOQ in at least some, and As, Co, Se, and Hg in all of the samples.

No particular temporal trend was observed during the two weeks, similar to most other pollutants. As a consequence of proximity to sources and local meteorological conditions, the atmospheric concentrations of individual anthropogenically mobilized elements in air may vary by 1–2 orders of magnitude between urban sites. The concentration levels found for most heavy metals in Salina Cruz were in the range of recent observations at Mexican [5, 17] and other Latin American (e.g. [18]) and European (e.g. [6, 8, 19–21]) urban sites, but below the levels found nowadays at urban sites in China (e.g. [22, 23]). The concentrations in the Salina Cruz aerosol were very close to background for K, Ca, Ti, Mn, Fe, and Sr (crustal enrichment factors, $EF_{crustal} = 1.2–1.5$), but clearly above background for Ni, Cu, Zn, As, Br, and Pb ($EF_{crustal} = 17–140$), as well as S and Se ($EF_{crustal} = 1000–3000$). Hereby, the concentration ratios to a reference element, Si, in the aerosol are compared with the same ratios in the crust, $EF_{crustal} = (c_i/c_{Si})_{aerosol}/(c_i/c_{Si})_{crustal}$ (following [24]; crustal composition was based as referenced in [25]). Pb ($<1.03\,ng\,m^{-3}$, $EF_{crustal} = 17$) was found to be particularly low, while V (on average 26 and reaching up to $152\,ng\,m^{-3}$, while at urban sites usually $<20\,ng\,m^{-3}$ is found; $EF_{crustal} = 43$) and Ni (by average 9.8 and reaching up to $44\,ng\,m^{-3}$, while commonly $<10\,ng\,m^{-3}$ is found; $EF_{crustal} = 29$) levels were found particularly elevated [21, 25]. Also, Br ($<1.2\,ng\,m^{-3}$; $EF_{crustal} = 140$) was particularly low compared with other urban sites. Besides, the $EF_{crustal}$ anthropogenic mobilization is also indicated by the Br : Cl ratio (0.65% by average), which exceeded the sea-salt Br : Cl ratio (0.34%). The Pb and non-sea-salt Br levels suggest that fuel additives, though insignificantly, still add to Pb and Br in air and the Pb levels at the site (Br : Pb = 0.4–0.5 in vehicular traffic emissions; cf [26, 27]) in agreement with a recent study in Mexico City [28]. The mobilization of As is usually mostly due to coal burning, which is probably not significant in the study area.

V has been identified to be on the rise in air in Mexico [29]. As the number of samples is very low for some of the elements, we refrain from any further conclusions.

Si, K, Ca, Ti, Mn, Fe, Rb, and Sr were highly and significantly correlated (on $\leq 0.5\%$ levels; $r > 0.7$). The occurrence of these elements was obviously (cf low $EF_{crustal}$ factors) dominated by wind erosion of soils and resuspension of dust. Wind velocity was weakly correlated ($r = 0.4–0.6$, i.e. significant on the 10% and 1% levels, respectively) with the levels of these elements. Besides wind, road traffic and construction activities in the city will have contributed to this source. Also, V and Ni (significantly correlated on $\leq 5\%$ levels; $r > 0.99$) and Br and Pb co-occurred (not significant). These elements, are known as tracers for oil combustion (V, Ni; e.g. [30, 31]) or vehicle traffic (Br, Pb; e.g. [27, 31]), respectively. Unlike most other elements, V was on average significantly more concentrated in air advected from the south (sea, harbour) than from the north (land and refinery; table 1). It was found to be correlated with sea salt (using Na^+ as a tracer [13]). Only in one case was an elevated V concentration observed when advection was

from the north to north-east (night-time sample 4–5 June, V determined) but this was found in two cases when advection from the south to south-west prevailed (daytime samples of 7 and 12 June) or under changing wind directions (daytime sample of 15 June). No such analysis was possible for Ni, Br, and Pb because of too few samples with positive determination of these elements. They were, however, anti-correlated with seasalt. The recirculation of polluted air masses originating from land is the reason for advection of polluted air from the sea. In fact, the sea breeze never brought clean air. In the case of V, elevated levels during advection from the south point to ships burning oil, offshore or in the harbour. Furthermore, oil tanks were located to the south and south-west in the harbour and 0.5–1 km to the west of the harbour. In conclusion, it is most likely that ships' emissions contributed to elevated V levels. These elements are well-known tracers for oil combustion (e.g. [32]). Elevated levels were observed in other harbour cities, Hong Kong and Athens, too, in the absence of major oil combustion plants [33, 34].

The dominant sources of Zn ($EF_{crustal} = 130$) and Cu ($EF_{crustal} = 74$) in air in Salina Cruz are not obvious. Their abundances in air are usually determined by more than one significant source type, various industries and road transport (e.g. [30, 35]). Such industries as smelting probably do not exist in the Isthmus region. Interestingly, we find that Cu and As are the only elements correlated with black carbon (BC; significant at the 5% level). BC was determined by local combustion sources, such as vehicles and the refinery. Ships might have contributed, too [12, 13]. Possibly, Cu was associated with combustion particles more than other heavy metals.

Daytime concentrations of particulate mass and of all elements exceeded night-time concentrations. The time-weighted mean exceedance was typically 10–100%, but much higher for some elements, i.e. V, Mn, Ni, Rb, Sr, and Hg (table 1). However, very high values result from a small database with some of the values below LOQ. Higher daytime concentrations point to stronger emissions during the day than during the night, eventually overcompensating for lower mixing during the night. The observations of daytime elevated V and Ni might indicate preferential daytime burning of oil in Salina Cruz. The same observations have been reported from an urban site in Germany [8]. On the other hand, the contrast between daytime and night-time is not independent of the direction of advection as this was mostly from the south (sea) during the daytime and mostly from the north (land) during the night-time as pointed out above. Most elements were higher concentrated in air from the sea. The same observation was reported for most inorganic ions and carbon fractions. Particulate matter mass (table 1), nitrate, and one organic carbon fraction [13], however, were higher concentrated in air from the north. Mass was 33% higher on average. Nitrate and organic carbon are dominated by secondary formation and, hence, regional transport. In this lack of coincidence with regionally distributed pollutants, we see an additional indication that the heavy metals were determined by local, rather than regional, sources. The primary emissions of the refinery were not reflected as higher levels from the north, because at least part of the time, the chain of small hills in the NE shielded the site from direct advection of the plume of the refinery. Then, the centre of the plume was elevated.

3.3 *Mass size distributions and effect of washout*

The concentrations for 13 elements, Si, Cl, K, Ca, Ti, V, Mn, Fe, Ni, Cu, Zn, Br, and Pb, in the size ranges 0.25–1.0 and 1–4 μm (stages 2 and 3 of the impactor) are listed

Table 2. Time-weighted mean elemental masses for stage 2/stage 3 (ng m^{-3}) during the entire campaign ($n = 23$), corresponding to the size intervals 0.25–1.0 and 1–4 of aerodynamic particle size, respectively.[a]

	All (n)	Days (n)	Nights (n)	No rain (n)	Rain (n)
Si	79/505 (16)	141/723 (7)	50/405 (9)	101/634 (11)	37/270 (5)
Cl	1/56 (10)	0.5/58 (4)	1.5/55 (6)	1/67 (7)	1/35 (3)
K	14/65 (17)	23/83 (8)	10/56 (9)	18/79 (12)	6/39 (5)
Ca	16/86 (13)	27/118 (6)	11/70 (7)	18/103 (9)	11/53 (4)
Ti	1.5/7.7 (14)	2.0/9.3 (5)	1.2/7.0 (8)	1.8/10.1 (11)	0.9/3.5 (3)
V	5.4/5.9 (13)	15/16 (5)	0.9/1.2 (7)	7.7/8.1 (9)	1.2/1.8 (4)
Mn	0.6/1.8 (16)	1.0/2.7 (7)	0.4/1.4 (8)	0.7/2.1 (11)	0.4/1.2 (5)
Fe	26/111 (17)	42/141 (7)	18/97 (9)	29/133 (12)	19/70 (5)
Ni	0.8/2.0 (9)	1.9/4.5 (3)	0.2/0.9 (6)	1.1/2.9 (7)	0.2/0.4 (2)
Cu	0.9/1.4 (8)	0.4/1.5 (2)	1.1/1.4 (6)	0.9/2.0 (6)	0.9/0.4 (2)
Zn	2.7/4.3 (13)	3.2/7.3 (6)	2.5/2.7 (7)	2.3/4.5 (8)	3.4/3.6 (4)
Br	0.09/0.13 (5)		0.13/0.19 (5)	0.10/0.09 (4)	0.08/0.19 (2)
Pb	0.22/0.19 (9)	0.29/0.19 (3)	0.19/0.19 (6)	0.24/0.23 (7)	0.20/0.11 (3)

[a]n = number of samples.

in table 2, while the complete mass size distributions of seven of these, Si, K, Ca, Ti, Mn, Fe, and Zn, are shown in figure 1 and for subsets of samples (corresponding to nights/prevailing northerly advection, days/prevailing southerly advection, no rain and rain, respectively) in tables 3 and 4.

On average, 3.5, 5.7, 8.7, and 1.7 μg m^{-3} of particulate matter mass was determined in size ranges corresponding to stages 4–1 (decreasing cutoffs) of the impactor, which means that 73% of the mass was associated with particles with an aerodynamic diameter of 0.25–4 μm. The mass size distributions of Si, Cl, K, Ca, Ti, V, Cr, Mn, Fe, Ni, Rb, and Sr exhibited their maximum in the size range 1–4 μm. The maximum of the mass size distribution of one element, Pb, is found in the sub-micrometre range corresponding to 0.25–1 μm (tables 2 and 3). Roughly equal masses in the 0.25–1 μm and 1–4 μm ranges are found for V and Br. Bimodality due to maxima in the second and fourth stages (corresponding to 0.25–1 and 4–16 μm, respectively) is found for Cu and Zn (tables 3 and 4). Note that the number of modes found in the mass size distribution cannot provide more than a lower limit for the true number due to the very coarse size resolution. For both elements, the mass size distribution found is in agreement with observations at European urban sites [35, 36].

Washout, dry removal, and aging are processes which change the mass size distributions: the mass median diameters (MMD; tables 3 and 4) are smaller in nighttime samples than in daytime samples by 0.8–1.4 μm. MMDs are smaller in samples with rain than in samples of dry intervals by 1.0–1.7 μm (tables 3 and 4, respectively). The latter is obviously a consequence of a higher washout efficiency of the large particles [37]. Among the seven elements with a complete mass size distribution, this effect was most pronounced for Mn and Zn (cf figure 1a and b). Large particles and water-soluble particles are removed preferentially, while small particles and hydrophobic matter (e.g. BC) will be largely preserved. This is reflected as a significant reduction in the mass mixing ratio in the particulate phase of those elements which are of crustal origin (including dust resuspension), Si, K, Ti, Mn, and Fe, by 16–31% (table 4). No significant respective changes are found for Ca and Zn. This complements the finding that Mg ions were enriched in rainwater, while Ca ions were not [13]. This, in turn, underscores that Ca, besides as mineral dust, is also carried in another aerosol type.

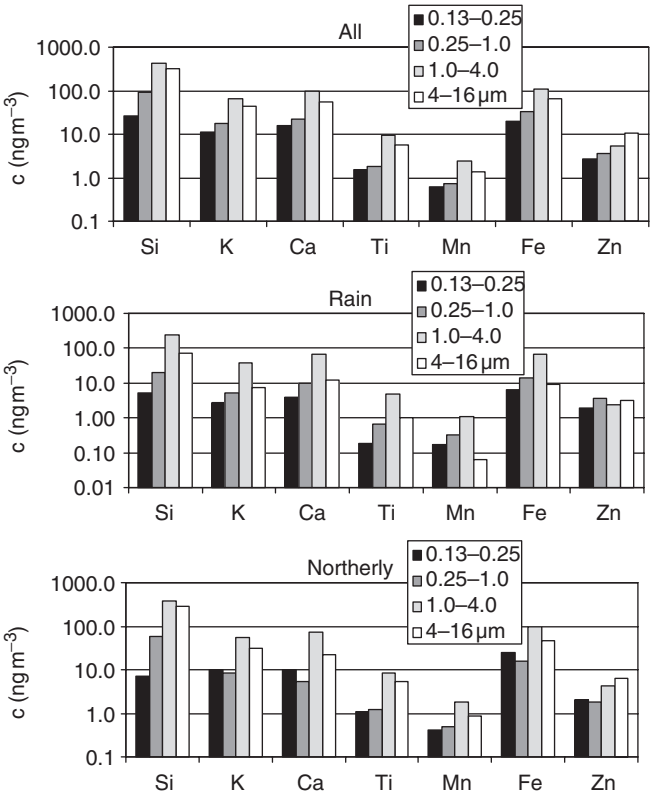

Figure 1. Mass size distributions of selected elements for (a) all sampling intervals and (b, c) subsets of samples.

The reduction in MMD in night-time samples and at the same time in samples representing advection from the north (table 3) can be explained by aging of the aerosol. In particular, the smallest particle size fraction, 0.13–0.25 µm, of K, Ca, Fe, and Zn was more prominent when advection was from the north (figure 1a and c). Aerosols advected from the south are mostly recirculated aerosols. The rhythm of land and sea breeze causes offshore travel distances of air masses around 100 km. During aging, the small particles had grown by coagulation or condensation. They had been removed only to a small extent [12]. The fraction of large particles had decreased, possibly due to sedimentation or washout. The difference is largest for Zn (−1.38 µm), the element whose mass size distribution exhibited the second maximum at 4–16 µm. The difference is smallest for V (−0.33 µm), the element which exhibited the largest concentration drop (−95%). The mass contribution of primary aerosols is decreasing during aging as secondary aerosols are formed. Unfortunately, no mass mixing ratio analysis is possible, as the size-segregated particulate matter mass data of the selected samples (table 3) are incomplete.

The effect of dry removal and re-distribution of particulate matter during transport can be best addressed by analysis of those air masses without precipitation which were sampled twice, namely during land breeze (northerly) and, during the subsequent sampling interval, under sea breeze (southerly). Respective data are available from two pairs of subsequent sampling intervals, namely on 13–14 and 14–15 June. The particulate matter mass concentrations had decreased in one case (13–14 June) and

Table 3. Time-weighted mean particulate matter and elemental mass size distributions during three selected days with southerly advection (7, 12, and 15 June) and three selected nights with northerly advection (6–7, 7–8, and 8–9 June).[a]

	Days/southerly		Nights/northerly			
	c	MMD	c	MMD	Δc	ΔMMD
Si	1259 (67/180/533/479)[b]	3.97	373 (11/27/255/80)	3.12	−70	−0.85
Cl			81 (2/2/65/12)	2.81		
K	234 (18/35/100/81)	3.71	65 (7/7/39/12)	2.75	−72	−0.96
Ca	378 (32/54/166/125)	3.62	101 (9/9/64/19)	2.83	−73	−0.79
Ti	30.1 (3.0/3.6/14/9.5)	3.53	7.8 (0.3/0.8/5.4/1.3)	2.78	−74	−0.76
V	80 (11/33/30/6)	1.58	4.3 (0.9/1.1/2.3/ <0.02)	1.25	−95	−0.33
Mn	9.8 (1.1/1.4/4.4/2.8)	3.31	1.9 (0.2/0.3/1.2/0.2)	2.20	−80	−1.11
Fe	377 (28/72/159/118)	3.46	97 (6/13/65/13)	2.49	−74	−0.97
Co			0.02 (0.02/ <0.003/ <0.003/ <0.003)[b]			
Ni			2.3 (0.5/0.4/0.9/0.5)	2.65		
Cu			12.1 (1.0/1.6/0.9/8.6)	5.92		
Zn	50 (5/8/11/27)	4.76	15.6 (3.0/3.2/4.1/5.3)	3.38	−69	−1.38
As			0.11 (0.01/0.06/0.04/ <0.003)	1.11		
Se			0.08 (0.01/0.05/0.03/ <0.003)[b]	1.08		
Br			0.8 (0.1/0.2/0.4/0.1)	2.15		
Pb	1.5 (0.2/0.7/0.3/0.3)[b]	2.26	0.7 (0.1/0.4/0.2/0.02)	1.08	−52	−1.18

[a]Data are given as total (stage 1/stage 2/stage 3/stage 4) concentrations, c (ng m^{-3}, except for m: μg m^{-3}), corresponding to the size intervals 0.13–0.25, 0.25–1.0, 1–4, and 4–16 μm of aerodynamic particle size, respectively, and the mass median diameter, MMD (μm). Δc, Δx and ΔMMD denote the differences in concentration (%), mass mixing ratio ($x = c/m$) (%), and MMD (μm) between nights/northerly and days/southerly or no rain and rain, respectively.
[b]$n = 2$.

Table 4. Time-weighted mean particulate matter and elemental mass size distributions during six sampling periods without rain and two with rain.[a]

	No rain		Rain				
	c	MMD	c	MMD	Δc	Δx	ΔMMD
m	28.8 (3.6/11.4/8.2/5.6)	2.36	8.5 (0.3/4.3/3.9/ <0.05)	1.17	−70		−1.19
Si	1076 (36/123/498/420)	4.11	336 (5/21/240/70)	3.13	−69	−24	−0.99
K	176 (15/23/77/60)	3.69	54 (3/5/39/7)	2.57	−69	−25	−1.12
Ca	233 (21/27/113/73)	3.54	92 (4/10/66/13)	2.58	−60	−3	−0.95
Ti	23.2 (2.1/2.3/11/7.7)	3.69	6.5 (0.2/0.7/4.7/1.0)	2.72	−72	−31	−0.96
Mn	6.7 (0.8/0.9/3.0/1.9)	3.33	1.6 (0.2/0.3/1.1/0.1)	1.75	−75	−42	−1.58
Fe	278 (26/40/127/86)	3.47	95 (6/15/66/9)	2.22	−66	−16	−1.24
Zn	26.1 (3.0/3.5/6.4/13)	4.65	11.2 (1.9/3.6/2.4/3.3)	2.95	−57	+5	−1.70

[a]Data are given as total (stage 1/stage 2/stage 3/stage 4) concentrations, c (ng m^{-3}, except for m: μg m^{-3}), corresponding to the size intervals 0.13–0.25, 0.25–1.0, 1–4, and 4–16 μm of aerodynamic particle size, respectively, and the mass median diameter, MMD (μm). Δc, Δx and ΔMMD denote the differences in concentration (%), mass mixing ratio ($x = c/m$) (%), and MMD (μm) between nights/northerly and days/southerly or no rain and rain, respectively.

increased in the other (14–15 June). These changes cannot be interpreted without information on the vertical mixing, which is not available. Consistently, for particulate matter mass (presented in Baumgardner [13]), Ca, and Fe (figure 2), we find that the mass fraction of particles in the 4–16 μm size range had increased at the expense of smaller particles during transport.

This could be due to the settling of large particles which in a plume over time become enriched in the lower atmospheric levels or, if the centre of the plume is aloft during

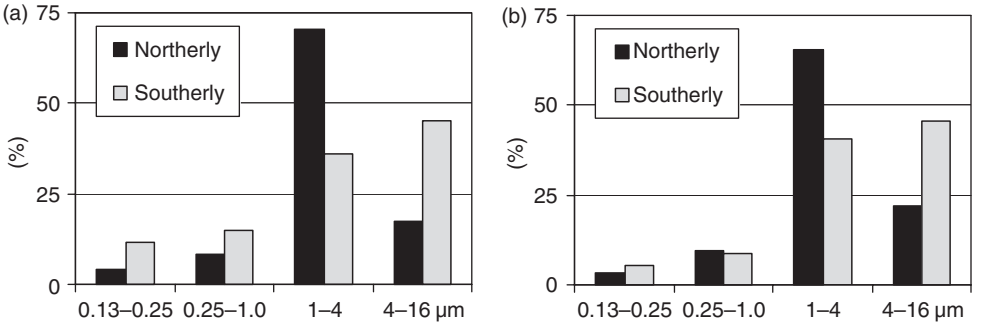

Figure 2. Relative mass size distributions of (a) Ca and (b) Fe for all sampling intervals ('all') and for two pairs of subsequent samples during 13–15 June, each with northerly followed by southerly (recirculated) advection.

southward transport, the vertical dispersion of the plume, or both. In any case, the conclusion is that during transport in the absence of precipitation, large particles become enriched in the near-ground aerosol.

During sampling intervals with rain particulate matter, mass concentrations were on average 38% lower than during dry sampling intervals. Most elements were more depleted by rain than particulate matter mass. Cu, Br, and Pb, however, were found at higher concentrations during sampling intervals with rain than without (table 1). The mass size distribution does not provide an explanation for this finding: Br and Pb had particularly low MMDs, while Cu had a particularly high MMD (table 3). This finding may be counterintuitive, but it is plausible, considering the limitations when interpreting time series: direct comparisons of data subsets (as done here) imply the assumption of horizontal homogeneity of the aerosol. This assumption is valid as long as source and sink processes can be neglected. The temporal variability of particulate matter mass and elemental concentrations, however, was considerable, which is common for urban sites (proximity to sources). Therefore, an apparent increase in concentrations in the data subset with rain events merely reflects the fact that temporal variability of sources and sinks overcompensates for the effect of the process being studied (washout). Still, this means that for these elements, Cu, Br, and Pb, the process being studied was less influential than for others.

4. Conclusions

4.1 *Sampling and analysis*

Using plastic sample supports as impaction plates in a cascade impactor, a simple method for direct determination of a number of elements in atmospheric particulate matter samples by TXRF was tested in an urban environment. Satisfactory LOQs were achieved, $<0.006\,\mathrm{ng\,m^{-3}}$ for Fe and Cu and $<0.002\,\mathrm{ng\,m^{-3}}$ for Si, Cl, K, Ca, Ti, V, Cr, Mn, Co, Ni, Zn, As, Se, Br, Rb, Sr, Hg, and Pb (for individual impactor stages) given

the choice of sample allocation (80% were reserved for other analyses) and time and particle size resolutions. This was due to the high variability in blank values (measured in the laboratory prior to exposure), even though many elements could not be determined in a number of samples. In future, this will be avoided by a more stringent criterion for rejection of supports after the blank measurement. Furthermore, tests showed that the initial coverage of the supports by a foil, not removed prior to the blank measurement, reduces the blank values.

For the study of atmospheric processes having characteristic times of hours (such as changes in atmospheric mixing and emission patterns), a higher time resolution and, for the investigation of particle dynamics, a higher size resolution (capable of dealing with 3–5 size modes) are desirable. Both requirements would considerably reduce the absolute analyte amounts per individual impactor stage to beyond the range accessible for TXRF. No high-volume size-segregating particulate-matter samplers which would allow sample focusing are available. Hence, an even more sensitive analysis method is required. A more intensive and more coherent excitation source promises a significant gain of sensitivity in XFA. Therefore, the development of a synchrotron-radiation-excited total reflection X-ray fluorescence spectrometry (SR-TXRF) method is in progress [38].

Apart from concentration and particle size (MMD), element speciation would be another property needed to fully assess heavy-metal-related human-health hazards. Other sensitive analysis methods are required and are in the process of being applied for aerosol analyses, such as X-ray absorption fine structure (XAFS [39, 40]) methods or plasma desorption mass spectrometry [18].

4.2 *Element cycling and health hazard*

As elements provide unique information on aerosol sources, the data reported here allowed complementary insights into the aerosol cycling in the polluted coastal environment being studied. In part, very low numbers of samples, 3–18 for individual elements, provide only a limited basis for assessment of the site's characteristics and for comparison with other environments.

Known sources have contributed to anthropogenically mobilized heavy metals. For V and Ni, which were found, elevated recirculation of local emissions as well as offshore emissions may have contributed. The risk of carcinogenesis from exposure to Ni as high as that measured in Salina Cruz ($9.8\,\mathrm{ng\,m^{-3}}$ on average) is about 2×10^{-6} [41]. Despite a very coarse size distribution (four size ranges), the elements' characteristic differences in mass size distributions and changes to the mass size distributions could be detected. Recirculation of the plume with the sea breeze allowed quasi-Lagrangian sampling from the same plume. Thereby, it was found that during transport in the absence of rain, the large particles became enriched in the near-ground aerosol. From a toxicological point of view, this is the less harmful alternative. The elements' mass associated with the small particles, on the other hand, was mostly preserved during the heavy precipitation events that the polluted air experienced during the studies. This suggests that even in the wet season in the humid subtropics, the main carriers of environmental health hazards have quite long atmospheric lifetimes.

Acknowledgements

We thank Hartmut Grassl, José Broekaert (Hamburg), and Graciela Raga (Mexico) for their active support of the study. The authors thank the Mexican Navy for permission to use the grounds of their Instituto de Investigaciones Oceanográficas and other support.

References

[1] C.A. Pope, M.J. Thun, M.N. Namboodiri, D.W. Dockery, J.S. Evans, F.E. Speizer, C.W. Heath. *Am. J. Respir. Crit. Care Med.*, **151**, 669 (1995).
[2] N. Künzli, R. Kaiser, S. Medina, M. Studnicka, O. Chanel, P. Filliger, M. Herry, F. Horak, V. Puybonnieux-Texier, P. Quenel, J. Schneider, R. Seethaler, J.C. Vergnaud, H. Sommer. *Lancet*, **356**, 795 (2000).
[3] H. Riveros-Rosas, G.D. Pfeifer, D.R. Lynam, J.L. Pedroza, A. Julian-Sanchez, O. Canales, J. Garfias. *Sci. Total Environ.*, **198**, 79 (1997).
[4] Joint World Health Organisation/Convention Task Force on the Health Aspects of Air Pollution. *Health Risks of Heavy Metals from Long-Range Transboundary Air Pollution*, WHO Regional Publications, European Series, Geneva (2006).
[5] J. Miranda, A. Andrade, A. Lopez-Suarez, R. Ledesma, T.A. Cahill, P.H. Wakabayashi. *Atmos. Environ.*, **30**, 3471 (1996).
[6] M. Vallius, T. Lanki, P. Tiittanen, K. Koistinen, J. Ruuskanen, J. Pekkanen. *Atmos. Environ.*, **37**, 615 (2003).
[7] R. Gieray, G. Lammel, G. Metzig, P. Wieser. *Atmos. Res.*, **30**, 263 (1993).
[8] A.C. John, T.A.J. Kuhlbusch, H. Fissan, K.G. Schmidt. *Spectrochim. Acta B*, **56**, 2137 (2001).
[9] K.R. Spurny. *Analytical Chemistry of Aerosols*, CRC Press, Boca Raton, FL (1999).
[10] R. Klockenkämper, A. von Bohlen. *Spectrochim. Acta B*, **44**, 461 (1989).
[11] M. Schmeling, R. Klockenkämper, D. Klockow. *Spectrochim. Chim. Acta B*, **52**, 985 (1997).
[12] D. Baumgardner, G.B. Raga, M. Grutter, G. Lammel. *Sci. Total Environ.*, **367**, 288 (2006).
[13] D. Baumgardner, G.B. Raga, M. Grutter, G. Lammel, M. Moya. *Sci. Total Environ.*, **372**, 287 (2006).
[14] R. Klockenkämper. *Total-Reflection X-Ray Fluorescence Analysis*, Wiley, New York (1997).
[15] P. Winkler. *J. Aerosol Sci.*, **5**, 235 (1974).
[16] R. Romero-Centeno, J. Zavala-Hidalgo, A. Gallegos, J.J. O'Brien. *J. Clim.*, **16**, 2628 (2003).
[17] F. Aldape, J. Flores, R.V. Diaz, J. Miranda, T.A. Cahill, J.R. Morales. *Int. J. PIXE*, **1**, 373 (1991).
[18] K.D. da Cunha, C.V.B. Leite. *Nucl. Instrum. Meth. Phys. Res.*, **187B**, 401 (2002).
[19] W. Maenhaut, J.L. Jaffrezo, R.E. Hillamo, T. Mäkelä, V.M. Kerminen. *Nucl. Instrum. Meth. Phys. Res. B*, **150**, 345 (1999).
[20] I. Salma, W. Maenhaut, E. Zemplén-Papp, G. Záray. *Atmos. Environ.*, **35**, 4367 (2001).
[21] G. Lammel, E. Brüggemann, T. Gnauk, K. Müller, C. Neusüss, A. Röhrl. *J. Aerosol Sci.*, **34**, 1 (2003).
[22] K.B. He, F.M. Yang, Y.L. Ma, Q. Zhang, X.H. Yao, C.K. Chan, S. Cadle, T. Chan, P. Mulawa. *Atmos. Environ.*, **35**, 4959 (2001).
[23] G. Lammel, Y.S. Ghim, J.A.C. Broekaert, H.W. Gao. *Fresenius Environ. Bull.*, **15**, 1539 (2006).
[24] K.A. Rahn. *Atmos. Environ.*, **10**, 597 (1976).
[25] R. Jaenicke. *Landolt-Börnstein Neue Serie*, **4b**, 391 (1988).
[26] G. Lammel. *Atmos. Environ.*, **29**, 3257 (1995).
[27] G. Lammel, A. Röhrl, H. Schreiber. *Environ. Sci. Poll. Res.*, **9**, 397 (2002).
[28] T. Martinez, J. Lartigue, F. Juarez, P. Avila-Perez, G. Zarazua, C. Marquez, M.P. Orta, V. Alvarez. *J. Atmos. Chem.*, **49**, 415 (2004).
[29] T.I. Fortoul, A. Quan-Torres, I. Sanchez, I.E. Lopez, P. Bizarro, M.L. Mendoza, L.S. Osorio, G. Espejel-Maya, M.D. Avila-Casado, M.R. Avila-Costa, L. Colin-Barenque, D.N. Villanueva, G. Olaiz-Fernandez. *Arch. Environ. Health*, **57**, 446 (2002).
[30] K. Coy, W. Dannecker, R. Henkelmann, H. Schreiber, H. Schwenke, H. Böddeker, J. Knoth, W. Bittner, U. Wätjen, H. Gross, K. Naumann, V. Krivan, K.H. Lieser, R. Neider, B.F. Schmitt, C. Segebade, M. Kühl, W. Michaelis, G. Tölg, H. Vogg. *Elementanalyse von Schwebstäuben*. Reports KfK-AFR006, KfK-AFR007, Karlsruhe, Germany (1983).
[31] D.G. Shendell, L.P. Naeher. *Environ. Int.*, **28**, 375 (2002).
[32] J.M. Pacyna. In *Toxic Metals in the Atmosphere*, J.O. Nriagu, C.I. Davidson (Eds), pp. 33–52, Wiley, New York (1986).

[33] Y.C. Lee, G. Calori, P. Hills, G.R. Carmichael. *Atmos. Environ.*, **36**, 1957 (2002).
[34] N.S. Thomaidis, E.B. Bakeas, P.A. Siskos. *Chemosphere*, **52**, 959 (2003).
[35] H. Horvath, M. Kasahara, P. Pesava. *J. Aerosol Sci.*, **27**, 417 (1996).
[36] H. Gerwig, H. Bittner, E. Brüggemann, T. Gnauk, H. Herrmann, G. Löschau, K. Müller. *Gefahrst. Reinh. Luft*, **66**, 175 (2006).
[37] H.R. Pruppacher, J.D. Klett. *Microphysics of Clouds and Precipitation*, Kluwer, Dordrecht, Netherlands (1997).
[38] U.E.A. Fittschen, S. Hauschild, M.A. Amberger, G. Lammel, C. Streli, S. Förster, P. Wobrauschek, C. Jokubonis, G. Pepponi, G. Falkenberg, J.A.C. Broekaert. *Spectrochim. Acta B*, **61**, 1098 (2006).
[39] J. Kawai, S. Tohno. *J. Trace Microprobe Techn.*, **19**, 497 (2001).
[40] S. Török, J. Osan, B. Beckhoff, G. Ulm. *Powder Diff.*, **19**, 81 (2004).
[41] US EPA, *Integrated Risk Informational System (IRIS), Database*, US EPA, Cincinnati, OH (1999). Available online at: http://www.epa.gov/iris/index.html (accessed 15 February 2007).